

Sequential Estimation of Gaussian Process-based Deep State-Space Models

Yuhao Liu, Marzieh Ajirak, and Petar M. Djurić, *Fellow, IEEE*

Abstract—We consider the problem of sequential estimation of the unknowns of state-space and deep state-space models that include estimation of functions and latent processes of the models. The proposed approach relies on Gaussian and deep Gaussian processes that are implemented via random feature-based Gaussian processes. With this model, we have two sets of unknowns, highly nonlinear unknowns (the values of the latent processes) and conditionally linear unknowns (the constant parameters of the random feature-based Gaussian processes). We present a method based on particle filtering where the constant parameters of the random feature-based Gaussian processes are integrated out in obtaining the predictive density of the states and do not need particles. We also propose an ensemble version of the method, with each member of the ensemble having its own set of features. With several experiments, we show that the method can track the latent processes up to a scale and rotation.

Index Terms—deep state-space models, deep Gaussian processes, sparse Gaussian processes, random features, ensembles, particle filtering, Bayesian linear regression

I. INTRODUCTION

In the last decade, the field of machine learning has seen an exceptional surge in progress backed up by unthinkable accomplishments. It is not an exaggeration to refer to this period as a revolution, with the primary enabler being a concept known as deep neural networks [1], [2].

The capabilities of deep neural networks are due to their structure, with multiple processing layers that can learn representations of data at various levels of abstraction [3], [4], [5]. The use of such networks has spread to a wide range of fields and now includes speech recognition [6], [7], visual object recognition [8], [9], object detection [10], [11], drug discovery [12], [13], and genomics [14], [15]. Even the field of physics has enthusiastically embraced deep networks [16], [17].

Gaussian processes (GPs) are now routinely employed in solving hard machine learning problems. The reason for this is that they provide a principled, practical, and probabilistic approach to learning [18]. Further, they are flexible, non-parametric, and computationally rather simple. They are used within a Bayesian framework that often leads to powerful methods which also offer valid estimates of uncertainties in predictions and generic model selection procedures [19]. Their main drawback of heavy computational scaling has recently been alleviated by the introduction of generic sparse approximations [20], [21], [22].

GPs have also been used for building dynamical models [23]. Because of their beneficial properties, including bias-variance trade-off and their Bayesian framework, they, too,

have become a tool for system identification [24]. The GP-based state-space models (GP-SSMs) describe dynamical systems by having one GP modeling a state process [25] and another GP modeling the function between the states and the observations or by a parametric structure [23].

If the functions are described by deep mappings such as deep GPs, the resulting model is referred to as a GP-based deep state-space model (GP-DSSM) [26]. A subclass of deep state-space models (DSSMs) can be built by extending variational autoencoders (VAEs) as in [27]. The building blocks for these models are recurrent neural networks (RNNs) and VAEs.

Recently, methods for probabilistic forecasting of time series based on RNNs have been proposed [28]. The objective was to learn complex patterns from raw data by an RNN combined with a parameterized per-time-series linear state-space model. Additional efforts with similar objectives and methodologies were reported in [29]. In [30], a global-local method based on deep factor models with random effects was explored. DSSMs were also used to construct deep GPs by hierarchically putting transformed GP priors on the length scales and magnitudes of the next level of GPs in the hierarchy [31]. All these methods are different from the ones we propose here.

One way of broadening the function space of a GP is by introducing an ensemble of GPs [32], [33], [34], [35]. Each GP may rely on all or on a subset of training samples and may use a unique kernel to make predictions. Ensembles of GPs have also been used for combining global approximants with local GPs [21], [36]. In [37], an ensemble of GPs was used for online interactive learning.

We address the problem of constructing dynamic deep probabilistic latent variable models. The underlying idea is that, unlike standard state-space models, we work with DSSMs, where the variables in the intermediate layers are independently conditioned on the variables from the deeper layers, and the dynamics are generated by the process from the deepest layer, the *root process*. An important task of inference is the estimation of the unknowns of the model, which include the underlying parameters of the GPs and the state (latent) processes of the model.

The contributions of the paper are as follows:

- a novel kernel-based method that identifies non-linear state-space systems without any information about the functions that govern the latent and observation processes,
- extension of the state-space models to deep structures to improve the model capacity and reveal more information about the studied phenomena,

- ensemble learning to reduce the variances of the estimates of the latent processes and the predictions of the observations.

II. BACKGROUND

In this section, we provide some background on methodologies that allow for a self-sustained presentation of the methods we propose in this paper.

A. Gaussian Processes

A GP, written as $\mathcal{GP}(m(\cdot), \kappa(\cdot, \cdot | \boldsymbol{\lambda}))$, is, in essence, a distribution over functions, where $m(\cdot)$ is a mean function, $\kappa(\cdot, \cdot)$ is a kernel or covariance function, and $\boldsymbol{\lambda}$ is a vector of hyper-parameters that parameterize the kernel. To simplify the notation, we express a GP as $\mathcal{GP}(m, \kappa)$ or as $\mathcal{GP}(m, \kappa(\boldsymbol{\lambda}))$, if $\boldsymbol{\lambda}$ is emphasized. For any set of inputs $\mathbf{X} = [\mathbf{x}_j]_{j=1}^J := [\mathbf{x}_1, \dots, \mathbf{x}_J]^\top$ in the domain of a real-valued function $f \sim \mathcal{GP}(m, \kappa)$, the function values $\mathbf{f} = [f(\mathbf{x}_j)]_{j=1}^J$ are Gaussian distributed, i.e.,

$$p(\mathbf{f} | \mathbf{X}) = \mathcal{N}(\mathbf{f} | \mathbf{m}_\mathbf{X}, \mathbf{K}_{\mathbf{X}\mathbf{X}}), \quad (1)$$

where $\mathbf{m}_\mathbf{X} = [m(\mathbf{x}_j)]_{j=1}^J$ is the mean and $\mathbf{K}_{\mathbf{X}\mathbf{X}} := \kappa(\mathbf{X}, \mathbf{X} | \boldsymbol{\lambda}) = [\kappa(\mathbf{x}_i, \mathbf{x}_j)]_{i,j}$. Given the observation \mathbf{f} on \mathbf{X} , the predictive distribution of \mathbf{f}^* at new inputs \mathbf{X}^* is given by [18]

$$p(\mathbf{f}^* | \mathbf{X}^*, \mathbf{f}, \mathbf{X}) = \mathcal{N}(\mathbf{f}^* | \boldsymbol{\mu}^*, \boldsymbol{\Sigma}^*), \quad (2)$$

with predictive mean and covariance obtained by

$$\begin{aligned} \boldsymbol{\mu}^* &= \mathbf{m}_{\mathbf{X}^*} + \mathbf{K}_{\mathbf{X}^*\mathbf{X}} \mathbf{K}_{\mathbf{X}\mathbf{X}}^{-1} (\mathbf{f} - \mathbf{m}_\mathbf{X}), \\ \boldsymbol{\Sigma}^* &= \mathbf{K}_{\mathbf{X}^*\mathbf{X}^*} - \mathbf{K}_{\mathbf{X}^*\mathbf{X}} \mathbf{K}_{\mathbf{X}\mathbf{X}}^{-1} \mathbf{K}_{\mathbf{X}\mathbf{X}^*}. \end{aligned} \quad (3)$$

B. Random Feature-Based Gaussian Processes

GPs do not scale up well with N , the number of input-output pairs. We observe that in (3), one has to invert the $N \times N$ matrix $\mathbf{K}_{\mathbf{X}\mathbf{X}}$, which for large values of N becomes an issue. To ameliorate the problem, we resort to approximations by exploiting the concept of sparsity. One approach to such an approximation is based on constructing GPs with features that come from a feature space [38].

Compared with approximations in a function space, a GP with a shift-invariant kernel has another way of approximation, one that focuses on a feature space. By utilizing feature spaces, the computations do not require matrix decompositions but only matrix multiplications. The vector of basis functions is comprised of trigonometric functions that are defined by

$$\boldsymbol{\phi}(\mathbf{x}) = \frac{1}{\sqrt{J}} [\sin(\mathbf{x}^\top \boldsymbol{\omega}^1), \cos(\mathbf{x}^\top \boldsymbol{\omega}^1), \dots, \sin(\mathbf{x}^\top \boldsymbol{\omega}^J), \cos(\mathbf{x}^\top \boldsymbol{\omega}^J)]^\top, \quad (4)$$

where $\boldsymbol{\Omega} = \{\boldsymbol{\omega}^j\}_{j=1}^J$ are random features sampled from the power spectral density of the kernel of the GP. Then the kernel function $k(\mathbf{x}, \mathbf{x}')$ can be approximated by $\boldsymbol{\phi}(\mathbf{x})^\top \boldsymbol{\phi}(\mathbf{x}')$ if the kernel is shift-invariant. It brings a type of GP approximation according to

$$f \approx \boldsymbol{\phi}(\mathbf{x})^\top \boldsymbol{\theta} \quad (5)$$

where $\boldsymbol{\theta}$ are parameters of the approximating model.

C. Bayesian Linear Regression

In view of the model given by (5), we provide a brief review of Bayesian linear regression. Consider the following model:

$$y = \boldsymbol{\phi}^\top \boldsymbol{\theta} + \epsilon, \quad (6)$$

where y is a scalar observation, ϵ is a zero-mean Gaussian random noise, i.e., $\epsilon \sim \mathcal{N}(0, \sigma^2)$, with σ^2 being unknown, $\boldsymbol{\phi} \in \mathbb{R}^{d_\theta \times 1}$ is a known feature vector, and $\boldsymbol{\theta} \in \mathbb{R}^{d_\theta}$ is an unknown parameter vector. We assume that $\boldsymbol{\theta}$ and σ^2 have a joint prior given by the multivariate normal-inverted Gamma distribution, i.e.,

$$p(\boldsymbol{\theta}, \sigma^2) \propto \frac{1}{\sigma^{a_0+1}} e^{-\frac{1}{2\sigma^2} (b_0 + (\boldsymbol{\theta} - \boldsymbol{\theta}_0)^\top \boldsymbol{\Sigma}_0^{-1} (\boldsymbol{\theta} - \boldsymbol{\theta}_0))}, \quad (7)$$

where $a_0, b_0, \boldsymbol{\theta}_0$, and $\boldsymbol{\Sigma}_0$ are parameters of the prior probability density function (pdf), and where $a_0 > d_\theta$ and $b_0 > 0$. One can show that the posterior predictive distribution of y is given by a Student's t -distribution [39],

$$p(y | \boldsymbol{\phi}, a_0, b_0, \boldsymbol{\theta}_0, \boldsymbol{\Sigma}_0) \propto \left(1 + \frac{1}{\varphi_1} (y - \boldsymbol{\phi}^\top \boldsymbol{\theta}_0)^2 \right)^{-\frac{\nu_1+1}{2}}, \quad (8)$$

where

$$\nu_1 = a_0 - d_\theta, \quad (9)$$

$$\varphi_1 = \frac{b_0}{1 - \boldsymbol{\phi}^\top \boldsymbol{\Sigma}_1^{-1} \boldsymbol{\phi}}, \quad (10)$$

$$\boldsymbol{\Sigma}_1 = (\boldsymbol{\Sigma}_0^{-1} + \boldsymbol{\phi} \boldsymbol{\phi}^\top)^{-1}. \quad (11)$$

Thus, for the linear model in (6), when the prior of $\boldsymbol{\theta}$ and σ^2 is given by (7), we have an analytical expression for the predictive distribution of y .

For the posterior of $\boldsymbol{\theta}$ and σ^2 we have

$$\begin{aligned} p(\boldsymbol{\theta}, \sigma^2 | y, \boldsymbol{\phi}, a_0, b_0, \boldsymbol{\theta}_0, \boldsymbol{\Sigma}_0) \\ \propto \frac{1}{\sigma^{a_1+1}} e^{-\frac{1}{2\sigma^2} (b_1 + (\boldsymbol{\theta} - \hat{\boldsymbol{\theta}}_1)^\top \boldsymbol{\Sigma}_1^{-1} (\boldsymbol{\theta} - \hat{\boldsymbol{\theta}}_1))}, \end{aligned} \quad (12)$$

where

$$a_1 = a_0 + 1, \quad (13)$$

$$b_1 = b_0 + y^2 + \boldsymbol{\theta}_0^\top \boldsymbol{\Sigma}_0^{-1} \boldsymbol{\theta}_0 - \hat{\boldsymbol{\theta}}_1^\top \boldsymbol{\Sigma}_1^{-1} \hat{\boldsymbol{\theta}}_1, \quad (14)$$

$$\boldsymbol{\theta}_1 = \boldsymbol{\Sigma}_1 (\boldsymbol{\Sigma}_0^{-1} \boldsymbol{\theta}_0 + \boldsymbol{\phi} y). \quad (15)$$

Clearly, the posterior pdf is also a multivariate normal-inverse Gamma pdf with parameters $a_1, b_1, \boldsymbol{\theta}_1$, and $\boldsymbol{\Sigma}_1$, which are updated from $a_0, b_0, \boldsymbol{\theta}_0$ and $\boldsymbol{\Sigma}_0$ using (13), (14), (15) and (11), respectively.

D. Particle Filtering

In the proposed approach, we will use concepts from particle filtering theory, and in this subsection, we provide the basics of it. In many signal processing problems, we aim at tracking a latent process $\mathbf{x}_t \in \mathbb{R}^{d_x}$ of a state-space model given by

$$\text{transition pdf: } p(\mathbf{x}_t | \mathbf{x}_{t-1}), \quad (16)$$

$$\text{likelihood of } \mathbf{x}_t: p(y_t | \mathbf{x}_t), \quad (17)$$

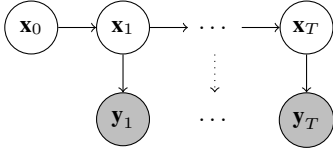


Fig. 1. A generic diagram of an SSM.

where t is a discrete-time index, and $y_t \in \mathbb{R}$ is an observation process. Typically, the main objective of PF is to obtain the filtering pdf $p(\mathbf{x}_t|y_{1:t})$ from $p(\mathbf{x}_{t-1}|y_{1:t-1})$.

In brief, particle filters approximate the pdfs of interest by discrete random measures, where the support of a pdf is given by a set of particles and where each particle is given a weight following fundamental principles. PF is implemented as follows [40]. Suppose that at time $t-1$ the filtering density $p(\mathbf{x}_{t-1}|y_{1:t-1})$ is approximated by

$$p^M(\mathbf{x}_{t-1}|y_{1:t-1}) = \frac{1}{M} \sum_{m=1}^M \delta(\mathbf{x}_{t-1} - \mathbf{x}_{t-1}^{(m)}), \quad (18)$$

where the symbol $\mathbf{x}_{t-1}^{(m)}$ represents the m th particle (sample) of \mathbf{x}_{t-1} , $\delta(\cdot)$ is the Dirac delta function, and M is the number of particles. Then we can obtain $p^M(\mathbf{x}_t|y_{1:t})$ from $p^M(\mathbf{x}_{t-1}|y_{1:t-1})$ by implementing three steps:

- 1) Generate particles $\mathbf{x}_t^{(m)}$ from the predictive pdf of \mathbf{x}_t . i.e.,

$$\mathbf{x}_t^{(m)} \sim p(\mathbf{x}_t|\mathbf{x}_{t-1}^{(m)}). \quad (19)$$

- 2) Compute the weights of the particles $\mathbf{x}_t^{(m)}$ according to the likelihood of \mathbf{x}_t , or

$$w_t^{(m)} \propto p(y_t|\mathbf{x}_t^{(m)}), \quad (20)$$

and where

$$\sum_{m=1}^M w_t^{(m)} = 1. \quad (21)$$

The approximation of $p(\mathbf{x}_t|y_{1:t})$ is then given by

$$p^M(\mathbf{x}_t|y_{1:t}) = \sum_{m=1}^M w_t^{(m)} \delta(\mathbf{x}_t - \mathbf{x}_t^{(m)}). \quad (22)$$

- 3) Resample the particles using their weights $w_t^{(m)}$ and construct a posterior of \mathbf{x}_t with equal weights and where some of the particles are replicated [41].

III. GAUSSIAN PROCESS STATE SPACE MODEL

Now we introduce the GP-based state space model. Suppose the observation process $\mathbf{y}_t \in \mathbb{R}^{d_y}$ is produced by a state-space model defined by

$$\mathbf{x}_t = f(\mathbf{x}_{t-1}) + \mathbf{u}_t, \quad (23)$$

$$\mathbf{y}_t = g(\mathbf{x}_t) + \mathbf{v}_t, \quad (24)$$

where (23) represents the latent state transition equation with the state vector $\mathbf{x}_t \in \mathbb{R}^{d_x}$ at time instant t , and (24) is the observation equation with $\mathbf{y}_t \in \mathbb{R}^{d_y}$ being the vector of observations at time instant t . The symbols $\mathbf{u}_t \sim \mathcal{N}(\mathbf{0}, \sigma_u^2 \mathbf{I})$

and $\mathbf{v}_t \sim \mathcal{N}(\mathbf{0}, \sigma_v^2 \mathbf{I})$ represent Gaussian distributed errors (noises). A generic graphical representation of an SSM is shown in Fig. 1.

Next, we express the above two equations using random feature-based GPs. In that case, we write them according to

$$\mathbf{x}_t = \mathbf{H}^\top \boldsymbol{\phi}^x(\mathbf{x}_{t-1}) + \mathbf{u}_t, \quad (25)$$

$$\mathbf{y}_t = \boldsymbol{\Theta}^\top \boldsymbol{\phi}^y(\mathbf{x}_t) + \mathbf{v}_t, \quad (26)$$

where the parameter variables are given by the elements of the matrices $\mathbf{H} \in \mathbb{R}^{2J_x \times d_x}$, $\mathbf{H} = [\boldsymbol{\eta}^{[1]}, \boldsymbol{\eta}^{[2]}, \dots, \boldsymbol{\eta}^{[d_x]}]$, and $\boldsymbol{\Theta} \in \mathbb{R}^{2J_y \times d_y}$, $\boldsymbol{\Theta} = [\boldsymbol{\theta}^{[1]}, \boldsymbol{\theta}^{[2]}, \dots, \boldsymbol{\theta}^{[d_y]}]$. Thus, each dimension of \mathbf{x}_t and \mathbf{y}_t is modeled by its own set of parameters. Further, note that the feature vectors $\boldsymbol{\phi}^x \in \mathbb{R}^{2J_x}$ and $\boldsymbol{\phi}^y \in \mathbb{R}^{2J_y}$ in (25) and (26) are different because they are defined by different sets of embedded random features $\boldsymbol{\Omega}^x$ and $\boldsymbol{\Omega}^y$, respectively. To simplify the notation, we use $\boldsymbol{\phi}^x(\mathbf{x}_{t-1}) =: \boldsymbol{\phi}_{t-1}^x$ and $\boldsymbol{\phi}^y(\mathbf{x}_t) =: \boldsymbol{\phi}_t^y$. We assume that the parameter variables are all independent, i.e., the columns of \mathbf{H} and $\boldsymbol{\Theta}$ are independent of the remaining columns. The noises \mathbf{u}_t and \mathbf{v}_t are i.i.d. zero-mean Gaussians, where $\mathbf{u}_t \sim \mathcal{N}(\mathbf{0}, \boldsymbol{\Sigma}_u)$ and $\mathbf{v}_t \sim \mathcal{N}(\mathbf{0}, \boldsymbol{\Sigma}_v)$, with $\boldsymbol{\Sigma}_u = \text{diag}(\sigma_u^{2[1]}, \sigma_u^{2[2]}, \dots, \sigma_u^{2[d_x]})$ and $\boldsymbol{\Sigma}_v = \text{diag}(\sigma_v^{2[1]}, \sigma_v^{2[2]}, \dots, \sigma_v^{2[d_y]})$.

The model described by (25) and (26) contains many unknowns, that is, the vector processes \mathbf{x}_t , $t = 1, 2, \dots$, the parameter matrices \mathbf{H} and $\boldsymbol{\Theta}$, and the noise variances $\sigma_u^{2[d]}$, $d = 1, 2, \dots, d_x$ and $\sigma_v^{2[d]}$, $d = 1, 2, \dots, d_y$. Conditioned on \mathbf{x}_t , the model is of the same form as the one in (6), whereas conditioned on \mathbf{H} and $\boldsymbol{\Theta}$, the model given by (25) and (26) is very nonlinear in \mathbf{x}_t . On account of the intractable analytical inference, we resort to PF to estimate sequentially the latent states. Given the estimated states, we update the respective joint distributions of \mathbf{H} and $\boldsymbol{\Sigma}_u$ as well as the one of $\boldsymbol{\Theta}$ and $\boldsymbol{\Sigma}_v$ by applying Bayesian linear regressions, where we use multivariate normal-inverse Gamma pdfs for the joint priors of $(\boldsymbol{\eta}^{[d]}, \sigma_u^{2[d]})$ and $(\boldsymbol{\theta}^{[d]}, \sigma_v^{2[d]})$, respectively.

Next, we explain how we implement the following:

- 1) the propagation of \mathbf{x}_t ,
- 2) the update of the joint posteriors of $\boldsymbol{\eta}^{(m),[d]}$ and $\sigma_u^{(m),[d]^2}$, for $d = 1, 2, \dots, d_x$, $m = 1, 2, \dots, M$,
- 3) the update of the joint posteriors of $\boldsymbol{\theta}^{(m),[d]}$ and $\sigma_v^{(m),[d]^2}$, for $d = 1, 2, \dots, d_y$, $m = 1, 2, \dots, M$, and
- 4) the weight computation of the particles and estimation of \mathbf{x}_t .

Suppose that before propagating the samples of the latent process at time $t-1$, we have M particles of \mathbf{x}_{t-1} , $\mathbf{x}_{t-1}^{(m)}$, $m = 1, 2, \dots, M$. Assume also that for each stream of particles m at $t-1$ we have the joint posterior of $\boldsymbol{\eta}^{[d]}$ and $\sigma_u^{2[d]}$, which is a multivariate normal-inverse Gamma pdf with parameters $a_{t-1}^x, b_{t-1}^{(m),[d]}, \boldsymbol{\eta}_{t-1}^{(m),[d]}$ and $\boldsymbol{\Psi}_{t-1}^{(m),[d]}$. Further, we have the joint posterior of $\boldsymbol{\theta}^{[d]}$ and $\sigma_v^{2[d]}$, which is also a multivariate normal-inverse Gamma pdf and with parameters $a_{t-1}^y, c_{t-1}^{(m),[d]}, \boldsymbol{\theta}_{t-1}^{(m),[d]}$ and $\boldsymbol{\Upsilon}_{t-1}^{(m),[d]}$.

A. Propagation of the particles

We generate the elements of the particles $\mathbf{x}_t^{(m)}$, $\mathbf{x}_t^{(m),[d]}$, from respective univariate Student's t -distributions given by

(see also (8))

$$p(x_t^{(m),[d]} | \mathbf{x}_{t-1}^{(m)}, \mathbf{Y}_{t-1}) \propto \left(1 + \frac{1}{\psi_t^{(m),[d]}} \left(x_t^{(m),[d]} - \alpha_t^{(m),[d]} \right)^2 \right)^{-\frac{\nu_{t-1}^x + 1}{2}}, \quad (27)$$

where $d = 1, 2, \dots, d_x$, $m = 1, 2, \dots, M$, and

$$\nu_{t-1}^x = a_{t-1}^x - 2J_x, \quad (28)$$

$$\alpha_t^{(m),[d]} = \phi_{t-1}^{x(m)\top} \boldsymbol{\eta}_{t-1}^{(m),[d]}, \quad (29)$$

$$\psi_t^{(m),[d]} = \frac{b_{t-1}^{(m),[d]}}{1 - \phi_{t-1}^{x(m)\top} \boldsymbol{\Psi}_t^{(m),[d]} \phi_{t-1}^{x(m)}}, \quad (30)$$

$$\boldsymbol{\Psi}_t^{(m),[d]} = \left(\boldsymbol{\Psi}_{t-1}^{(m),[d]-1} + \phi_{t-1}^{x(m)} \phi_{t-1}^{x(m)\top} \right)^{-1}. \quad (31)$$

Thus, the propagation includes generating particles \mathbf{x}_t by (27). For each dimension of \mathbf{x}_t , we sample M particles (thus, we have a total of Md_x particles), and they represent the support of \mathbf{x}_t . Next is the evaluation of each of the particles. This is described in the next subsection.

B. Updating of the joint posteriors of $(\boldsymbol{\eta}^{(m),[d]}, \sigma_u^{(m),[d]2})$

The joint posterior of $(\boldsymbol{\eta}^{(m),[d]}, \sigma_u^{(m),[d]2})$ is a multivariate normal-inverted Gamma pdf with parameters $a_t^x, b_t^{(m),[d]}, \boldsymbol{\eta}_t^{(m),[d]}$, and $\boldsymbol{\Psi}_t^{(m),[d]}$. We update $\boldsymbol{\Psi}_{t-1}^{(m),[d]}$ by (31), and we find the remaining parameters recursively by

$$a_t^x = a_{t-1}^x + 1, \quad (32)$$

$$b_t^{(m),[d]} = b_{t-1}^{(m),[d]} + \left(x_t^{(m),[d]} \right)^2 + \boldsymbol{\eta}_{t-1}^{(m),[d]\top} \boldsymbol{\Psi}_{t-1}^{(m),[d]-1} \boldsymbol{\eta}_{t-1}^{(m),[d]} - \boldsymbol{\eta}_t^{(m),[d]\top} \boldsymbol{\Psi}_t^{(m),[d]-1} \boldsymbol{\eta}_t^{(m),[d]}, \quad (33)$$

$$\boldsymbol{\eta}_t^{(m),[d]} = \boldsymbol{\Psi}_t^{(m),[d]} \left(\boldsymbol{\Psi}_{t-1}^{(m),[d]-1} \boldsymbol{\eta}_{t-1}^{(m),[d]} + \phi_{t-1}^{x(m)} x_t^{(m),[d]} \right). \quad (34)$$

C. Updating of the joint posteriors of $(\boldsymbol{\theta}^{(m),[d]}, \sigma_v^{(m),[d]2})$

The proposed method also requires updating of the joint posteriors of $\boldsymbol{\theta}^{(m),[d]}$ and $\sigma_v^{(m),[d]2}$ for $m = 1, 2, \dots, M$, and $d = 1, 2, \dots, d_y$. The joint posterior of $(\boldsymbol{\eta}^{(m),[d]}, \sigma_u^{(m),[d]2})$ is a multivariate normal-inverted Gamma pdf with parameters $a_t^y, c_t^{(m),[d]}, \boldsymbol{\eta}_t^{(m),[d]}$, and $\boldsymbol{\Upsilon}_t^{(m),[d]}$. Upon receiving \mathbf{y}_t , these parameters are updated by

$$a_t^y = a_{t-1}^y + 1, \quad (35)$$

$$c_t^{(m),[d]} = c_{t-1}^{(m),[d]} + \left(y_t^{[d]} \right)^2 + \boldsymbol{\theta}_{t-1}^{(m),[d]\top} \boldsymbol{\Upsilon}_{t-1}^{(m),[d]-1} \boldsymbol{\theta}_{t-1}^{(m),[d]} - \boldsymbol{\theta}_t^{(m),[d]\top} \boldsymbol{\Upsilon}_t^{(m),[d]-1} \boldsymbol{\theta}_t^{(m),[d]}, \quad (36)$$

$$\boldsymbol{\theta}_t^{(m),[d]} = \boldsymbol{\Upsilon}_t^{(m),[d]} \left(\boldsymbol{\Upsilon}_{t-1}^{(m),[d]-1} \boldsymbol{\theta}_{t-1}^{(m),[d]} + \phi_t^{y(m)} y_t^{[d]} \right), \quad (37)$$

$$\boldsymbol{\Upsilon}_t^{(m),[d]} = \left(\boldsymbol{\Upsilon}_{t-1}^{(m),[d]-1} + \phi_t^{y(m)} \phi_t^{y(m)\top} \right)^{-1}. \quad (38)$$

D. Weight computation of particles and estimation of \mathbf{x}_t

We need to assign weights to each particle $\mathbf{x}_t^{(m)}$ according to the likelihood of $\mathbf{x}_t^{(m)}$. The computation proceeds according to

$$\tilde{w}_t^{(m)} = p(\mathbf{y}_t | \mathbf{x}_t^{(m)}, \mathbf{X}_{t-1}^{(m)}, \mathbf{Y}_{t-1}), \quad (39)$$

where $p(\mathbf{y}_t | \mathbf{x}_t^{(m)}, \mathbf{X}_{t-1}^{(m)}, \mathbf{Y}_{t-1})$ is the likelihood of $\mathbf{x}_t^{(m)}$ given \mathbf{y}_t , $\mathbf{X}_{t-1}^{(m)}$, and \mathbf{Y}_{t-1} , and where $\mathbf{X}_{t-1}^{(m)}$ represents all the particles generated in the m th stream up to time instant $t-1$, \mathbf{Y}_{t-1} stands for all the vector observations up to time instant $t-1$, and $\tilde{w}_t^{(m)}$ is the non-normalized weight of $\mathbf{x}_t^{(m)}$.

We obtain the likelihood by exploiting (26), where we use the made assumption that \mathbf{v}_t is Gaussian. We find that $p(\mathbf{y}_t | \mathbf{x}_t^{(m)}, \mathbf{X}_{t-1}^{(m)}, \mathbf{Y}_{t-1})$ is a product of d_y Student's t -distribution, i.e.,

$$p(\mathbf{y}_t | \mathbf{x}_t^{(m)}, \mathbf{X}_{t-1}^{(m)}, \mathbf{Y}_{t-1}) \propto \prod_{d=1}^{d_y} \left(1 + \frac{1}{v_t^{(m),[d]}} \left(y_t^{[d]} - \beta_t^{(m),[d]} \right)^2 \right)^{-\frac{\nu_{t-1}^y + 1}{2}}, \quad (40)$$

where $d = 1, 2, \dots, d_y$, $m = 1, 2, \dots, M$, and

$$\nu_{t-1}^y = a_{t-1}^y - 2J_y, \quad (41)$$

$$\beta_t^{(m),[d]} = \phi_t^{y(m)\top} \boldsymbol{\theta}_{t-1}^{(m),[d]}, \quad (42)$$

$$v_t^{(m),[d]} = \frac{c_{t-1}^{(m),[d]}}{1 - \phi_t^{y(m)\top} \boldsymbol{\Upsilon}_t^{(m),[d]} \phi_t^{y(m)}}. \quad (43)$$

Once we compute the non-normalized weights by (39), we normalize them according to

$$w_t^{(m)} = \frac{\tilde{w}_t^{(m)}}{\sum_{k=1}^M \tilde{w}_t^{(k)}}. \quad (44)$$

After normalizing the weights, the minimum mean square estimate (MMSE) of \mathbf{x}_t is estimated by

$$\hat{\mathbf{x}}_t = \sum_{m=1}^M w_t^{(m)} \mathbf{x}_t^{(m)}. \quad (45)$$

The approximation of the posterior $p(\mathbf{x}_t | \mathbf{Y}_t)$ is made by

$$p^M(\mathbf{x}_t | \mathbf{Y}_t) = \sum_{m=1}^M w_t^{(m)} \delta(\mathbf{x}_t - \mathbf{x}_t^{(m)}). \quad (46)$$

Finally, we resample M particles $\mathbf{x}_t^{(m)}$ from $p^M(\mathbf{x}_t | \mathbf{Y}_t)$ to obtain the particles that will be used for propagation in the next time instant $t+1$.

The complete procedure is summarized by Algorithm 1. We point out that an alternative algorithm can be applied where all the particles share the same parameters \mathbf{H} and $\boldsymbol{\Theta}$.

IV. ENSEMBLE LEARNING

The use of only a single set of random features $\boldsymbol{\Omega}$ might not be sufficiently accurate. In order to mitigate the problem, we introduce an ensemble of different sets of $\boldsymbol{\Omega}$ and then combine the results obtained by each set. Let $\boldsymbol{\Omega}^s$ be the s th set of pre-selected parameters $\boldsymbol{\Omega}$, and let its posterior contribution or weight to the overall estimate of the latent state be $w_t^s \propto$

Algorithm 1: Single Sequential GP-SSM

for $m = 1$ **to** M **do**

Sample $\mathbf{x}_1^{(m)} \sim p(\mathbf{x}_1)$;

Initialize the weights of $\mathbf{x}_1^{(m)}$ as $w_1^{(m)} = 1/M, \forall m$;

for $t = 2$ **to** T **do**

Propagation of the states:

Sample $\mathbf{x}_t^{(m)}$ according to (27);

Updating the parameters of the joint posterior of $(\boldsymbol{\eta}^{(m),[d]}, \sigma_u^{(m),[d]^2})$:

Update $a_t^x, b_t^{(m),[d]}, \boldsymbol{\eta}_t^{(m),[d]}$, and $\boldsymbol{\Psi}_t^{(m),[d]}$ via (32), (33), (34), and (31), $\forall d$ and m ;

Updating the parameters of the joint posterior of $(\boldsymbol{\theta}^{(m),[d]}, \sigma_v^{(m),[d]^2})$:

Update $a_t^y, c_t^{(m),[d]}, \boldsymbol{\theta}_t^{(m),[d]}$, and $\boldsymbol{\Upsilon}_t^{(m),[d]}$ via (35), (36), (37), and (38), $\forall d$ and m ;

Weight computation and normalization:

Compute the weights of $\mathbf{x}_t^{(m)}$ according to (39) and normalize them by (44).

Estimation of the state:

Estimate \mathbf{x}_t by (45).

Resampling:

Resample $\mathbf{x}_t^{(m)}$ based on their weights.

$p(s|\mathbf{Y}_t)$ at time t . Then, the predictive density of \mathbf{y}_t at time t is obtained from

$$\begin{aligned} p(\mathbf{y}_t|\mathbf{Y}_{t-1}) &= \sum_{s=1}^S p(s|\mathbf{Y}_{t-1})p(\mathbf{y}_t|s, \mathbf{Y}_{t-1}) \\ &= \sum_{s=1}^S w_{t-1}^s p(\mathbf{y}_t|s, \mathbf{Y}_{t-1}), \end{aligned} \quad (47)$$

where S is the total number of sets and where the posterior weight is updated by

$$w_t^s = \frac{p(s|\mathbf{Y}_{t-1})p(\mathbf{y}_t|s, \mathbf{Y}_{t-1})}{p(\mathbf{y}_t|\mathbf{Y}_{t-1})} \propto w_{t-1}^s p(\mathbf{y}_t|s, \mathbf{Y}_{t-1}). \quad (48)$$

A. Ensemble Estimates of the States

The ensemble estimate of the latent states is given by the mixture

$$p(\hat{\mathbf{x}}_t|\mathbf{Y}_t) = \sum_{s=1}^S w_t^s p(\hat{\mathbf{x}}_t|s, \mathbf{Y}_t). \quad (49)$$

We point out that the estimates of the latent states by random feature-based methods are identifiable up to a scale, shift, and rotation [42]. Thus, to fuse the state estimates, we have to force the estimators of all the ensemble members into the same coordinate base. To that end, we arbitrarily fix the rotation of $\mathbf{X} \in \mathbb{R}^{T \times d_x}$ by taking the singular value decomposition (SVD) of the MMSE estimate, $\hat{\mathbf{X}} = \mathbf{U}\mathbf{S}\mathbf{V}^\top$, and setting the new estimated $\hat{\mathbf{X}} \in \mathbb{R}^{T \times d_x}$ as the columns of the left singular vectors \mathbf{U} with d_x largest singular values. Then we mirror and rotate all the candidate latent states so that they have the same pattern. First, we set a guidance point $\tilde{\mathbf{x}}_t$ with respect to a specific time t . Then we rotate all the latent states $\tilde{\mathbf{X}}^{(s)}$ to

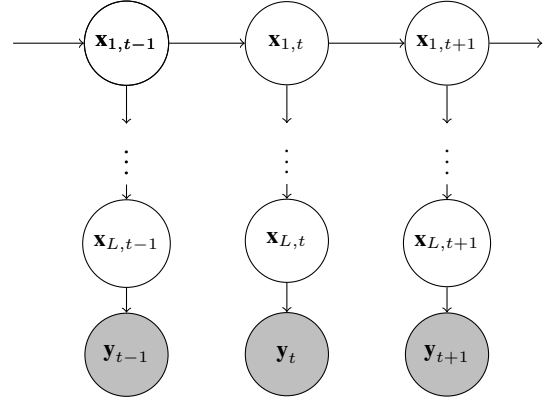


Fig. 2. A generic diagram of a deep SSM with L layers.

make sure that $\tilde{\mathbf{x}}_t^{(s)}$ is “overlapped” with $\tilde{\mathbf{x}}_t$. Finally, we take the weighted average of $\tilde{\mathbf{X}}^{(s)}$ as the ensemble estimate of $\tilde{\mathbf{X}}$.

B. Keep and Drop

We use the individual estimates of the ensemble members to improve on their respective estimates. In practice, if we do not take precautionary measures, only a small portion of them would remain with significant weights. For this reason, we remove the members with small weights using the principle of resampling and replace them with members that perform much better. With replacements, we reduce the diversity of features in the ensemble but increase the number of particles that explore the spaces of the latent processes with the features of the replicated members. Further, we note that candidate models need to be trained at the beginning. For this stage, we fix the weights to $w_t^s \equiv 1/S$ at the beginning until $t = T_0$.

V. GAUSSIAN PROCESS-BASED DEEP STATE-SPACE MODELS

One of the advantages of deep structures is to use one or a few simple nonlinear activation functions to improve the approximation of unknown highly nonlinear target functions. In the field of signal processing, the advantage of deep structures of state-space models is that with more hidden layers we can improve the modeling capacity of the model. Typically, the state processes of the hidden layers will be of different dimensions, and in some settings, the deep models can be justified using arguments that reflect our understanding of the phenomena we model. A generic diagram of a deep SSM with L layers is shown in Fig. 2.

Borrowing from concepts of deep learning, we introduce a Gaussian process-based deep state-space model (GP-DSSM). This model uses one simple kernel that is combined with a deep structure to approximate the unknown target kernel. Formally, we express a GP-DSSM with L hidden layers as follows:

$$\mathbf{x}_{1,t} = \mathbf{H}_1^\top \boldsymbol{\phi}_{1,t-1}^x + \mathbf{u}_{1,t}, \quad (50)$$

$$\mathbf{x}_{l,t} = \mathbf{H}_l^\top \boldsymbol{\phi}_{l,t}^x + \mathbf{u}_{l,t}, \quad l = 2 \dots, L, \quad (51)$$

$$\mathbf{y}_t = \boldsymbol{\Theta}^\top \boldsymbol{\phi}_t^y + \mathbf{v}_t, \quad (52)$$

where $\mathbf{x}_{l,t} \in \mathbb{R}^{d_x}$, $l = 1, 2, \dots, L$ are latent processes, $\mathbf{y}_t \in \mathbb{R}^{d_y}$ is a vector of observations, $\phi_{l,t}^x = \phi(\mathbf{x}_{l,t})$ are the feature functions embedded with different Ω_l for every layer, ϕ_t^y has the same meaning as before, \mathbf{H}_l and Θ are parameter variables, and $\mathbf{u}_{l,t}$ and \mathbf{v}_t are perturbations. We refer to the deepest latent process (defined by (50)) as the root process of the model. Here we assume that the dimensions of the latent processes are predefined. The objective of inference is to estimate all the latent processes $\mathbf{x}_{l,t}$, $l = 1, \dots, L$ and all the parameters of the model \mathbf{H} and Θ_l , $l = 1, 2, \dots, L$.

The inference method and procedures are very similar to the method we described for the ordinary GP-SSM.

A. Propagation of the particles in all layers

At time t , first we propagate the particles from $\mathbf{x}_{1,t-1}^{(m)}$ to $\mathbf{x}_{1,t}^{(m)}$ and then the particles of the remaining latent processes $\{\mathbf{x}_{l,t}^{(m)}\}_{l=2}^L$. In propagating these particles, we apply analogous Student's t -distributions as in (8), i.e.,

$$p(x_{l,t}^{(m),[d]} | \mathbf{X}_{t-1}^{(m)}, \mathbf{Y}_{t-1}) \propto \left(1 + \frac{1}{\psi_{l,t}^{(m),[d]}} \left(x_{l,t}^{(m),[d]} - \alpha_{l,t}^{(m),[d]} \right)^2 \right)^{-\frac{\nu_{l,t}^{(m),[d]} + 1}{2}}, \quad (53)$$

where $\mathbf{X}_{t-1}^{(m)}$ represents the latent states in all the layers up to time $t-1$, and where the parameters $\nu_{l,t}$, $\psi_{l,t}$, and $\alpha_{l,t}$ are defined similarly as in (28) – (31).

B. Updating of the joint posteriors of $(\eta_l^{(m),[d]}, \sigma_{l,v}^{(m),[d]^2})$ and $(\theta^{(m),[d]}, \sigma_v^{(m),[d]^2})$

These updates follow the schemes described by (32)–(34) and (35)–(38), respectively. We note that these updates can be performed in parallel once all the particles in all the layers have been propagated.

C. Weight computation of particles and estimation of the latent processes

We assign weights to the particles $\mathbf{x}_{l,t}^{(m)}$ according to the likelihoods of the particles, that is, we use

$$\tilde{w}_t^{(m)} = p(\mathbf{y}_t | \mathbf{x}_{L,t}^{(m)}, \mathbf{X}_{t-1}^{(m)}, \mathbf{Y}_{t-1}), \quad (54)$$

where $p(\mathbf{y}_t | \mathbf{x}_{L,t}^{(m)}, \mathbf{X}_{t-1}^{(m)}, \mathbf{Y}_{t-1})$ is the likelihood of $\mathbf{x}_{L,t}^{(m)}$ given \mathbf{y}_t , $\mathbf{X}_{t-1}^{(m)}$, \mathbf{Y}_{t-1} , and $\tilde{w}_t^{(m)}$, is again the non-normalized weight of $\mathbf{x}_{L,t}^{(m)}$. The computation of this weight is carried out via a Student's t -distribution of the form as in (40) and whose parameters are from expressions analogous to (41)–(43). Upon the computation of the weights, we normalize them as per (44). Clearly, these weights *directly* depend on $\mathbf{x}_{L,t}^{(m)}$ only and not on the particles from the previous layers. Finally, the minimum mean square estimate (MMSE) of $\mathbf{x}_{l,t}$ s are computed by (45) and the approximation of the posterior $p(\mathbf{x}_t | \mathbf{Y}_y)$ is given by (46). We reiterate that before we proceed to process the next observation, we resample the M streams using the weights $w_t^{(m)}$.

An alternative approach to computing the weights would be based on the following expressions

$$\tilde{w}_t^{(m)} = p(\mathbf{y}_t | \mathbf{x}_{L,t}^{(m)}, \mathbf{Y}_{t-1}) \prod_{l=1}^{L-1} p(\mathbf{x}_{l+1,t} | \mathbf{x}_{l,t}^{(m)}). \quad (55)$$

The problem in implementing (55) is that we do not know the latent processes $\mathbf{x}_{l,t}$. As a substitute of the unknown $\mathbf{x}_{l,t}$ s, we could use their respective MMSE estimates $\hat{\mathbf{x}}_{l,t}$ or even better, we could approximate the factors $p(\mathbf{x}_{l+1,t} | \mathbf{x}_{l,t}^{(m)})$ in (55) with the average likelihood, that is, with

$$p(\mathbf{x}_{l+1,t} | \mathbf{x}_{l,t}^{(m)}) \approx \sum_{m'=1}^M w_{l+1,t}^{(m')} p(\mathbf{x}_{l+1,t}^{(m')} | \mathbf{x}_{l,t}^{(m)}), \quad (56)$$

where $w_{l+1,t}^{(m')}$ are the weights associated with the particles $\mathbf{x}_{l+1,t}^{(m')}$. Thus, the process starts by computing the particles of $\mathbf{x}_{L,t}$, $w_{L,t}^{(m)}$. These weights and particles are then used to compute the weights of $\mathbf{x}_{L-1,t}$, $w_{L-1,t}^{(m)}$, and so on.

VI. EXPERIMENTS

We tested the performance of the proposed method with several experiments. In all the experiments, we applied the ensemble method with 100 members. Specifically, the random feature sets $\{\Omega^s\}_{s=1}^{100}$ were randomly sampled from the power spectral density of RBF kernels $\kappa^s(\lambda)$ with prior length scale vectors \mathbf{l}_λ^s and prior variances $\sigma_\lambda^2 = 1$, where the elements of \mathbf{l}_λ^s were independently sampled from the discrete set $\{10^{-4}, 10^{-3}, \dots, 10^3, 10^4\}$.

A. A test with $d_x = 2$ and $d_y = 1$

In the first experiment, we tested the inference of a GP-SSM when $d_x > d_y$. More specifically, we generated data from an SSM with $d_x = 2$ and $d_y = 1$ according to the following model:

$$\begin{aligned} \text{Latent Layer : } x_t^{[1]} &= 0.9x_{t-1}^{[1]} + 0.5\sin(x_{t-1}^{[2]}) + u_t^{[1]}, \\ x_t^{[2]} &= 0.5\cos(x_{t-1}^{[1]}) + 0.9x_{t-1}^{[2]} + u_t^{[2]}, \end{aligned}$$

$$\begin{aligned} \text{Observations : } y_t &= 0.3\sin(x_t^{[1]}) - 0.3x_t^{[1]} + 0.2x_t^{[2]} \\ &+ 0.25x_t^{[1]}x_t^{[2]} + (0.05x_t^{[1]})^2 + 0.01(x_t^{[1]})^3 \\ &- 0.25x_t^{[1]}/(1 + (x_t^{[2]})^2) + v_t. \end{aligned}$$

The generated data set contained 2,000 samples with $\sigma_u^2 = \sigma_v^2 = 0.001$, and for initializing the estimation, we used $T_0 = 1,000$ samples. For drawing random vectors needed in the construction of the random features $\phi(\mathbf{x})$ in (4), we used $J_x = J_y = 50$. Figures 3 and 4 show the last 100 samples of the actual latent processes $x_t^{[j]}$ and their estimates $\hat{x}_t^{[j]}$, respectively. For comparison purposes, all the signals were normalized from $T_0 = 1,000$ to $T = 2,000$. We emphasize again that the functions in the state and observation equations are unknown. The results suggest that with our approach we can capture the dynamics of the latent states. Recall from Section IV-A that we use the SVD to standardize both the actual and estimated states. Figure 5 illustrates the

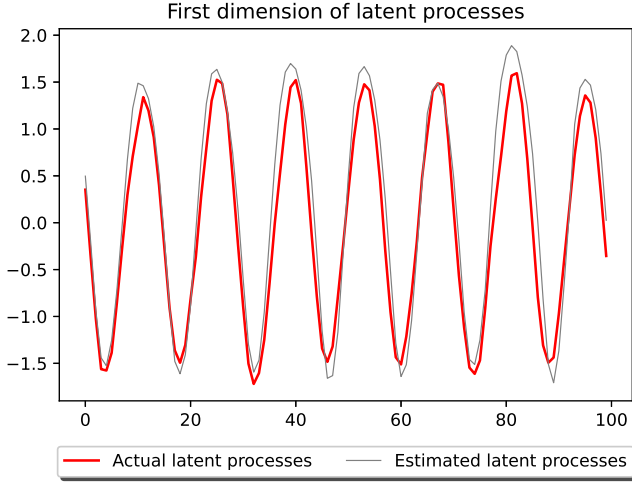


Fig. 3. The estimate of $\hat{x}_t^{[1]}$ and its true values $x_t^{[1]}$.

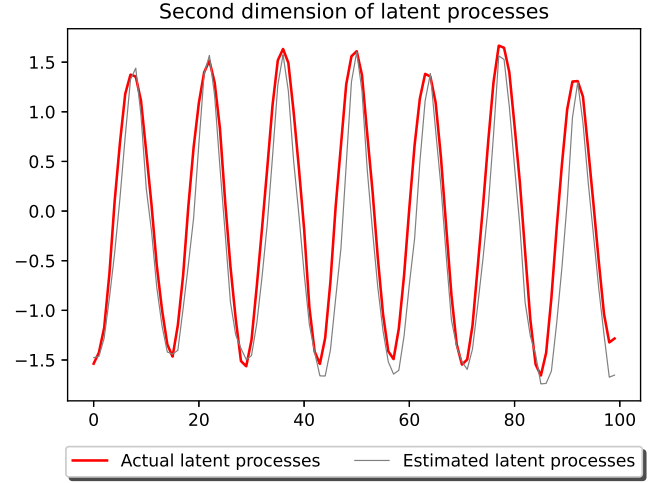


Fig. 4. The estimate of $\hat{x}_t^{[2]}$ and its true values $x_t^{[2]}$.

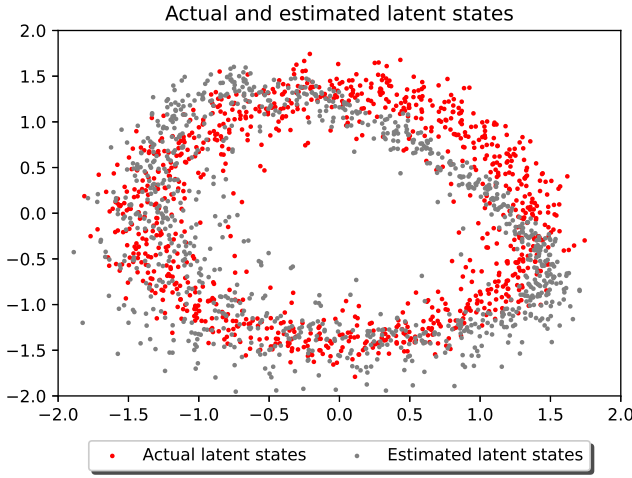


Fig. 5. Pairs of estimated ($\hat{\mathbf{x}}_t$) and actual (\mathbf{x}_t) latent states before SVD.

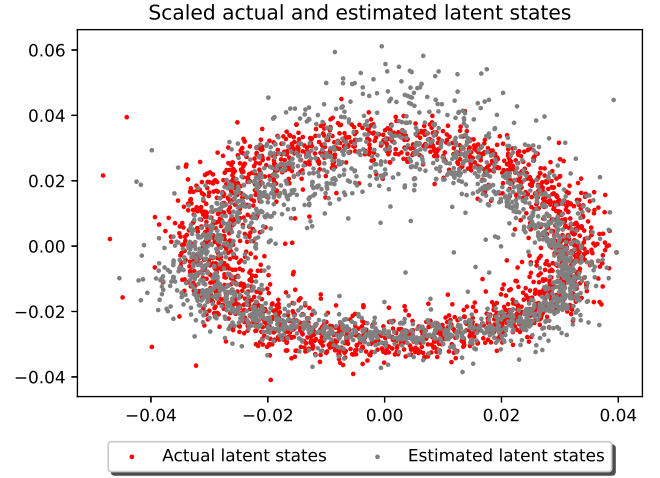


Fig. 6. Pairs of standardized $\hat{\mathbf{x}}_t$ and \mathbf{x}_t after SVD.

true pairs $(x_t^{[1]}, x_t^{[2]})$ and estimated pairs $(\hat{x}_t^{[1]}, \hat{x}_t^{[2]})$ before applying SVD. The new actual and estimated states after SVD are shown in Fig. 6.

B. A test with $d_x = 1$ and $d_y = 10$

In the next experiment, we tested the GP-SSM when $d_x < d_y$. We wanted to demonstrate the ability of our model to learn lower dimensional processes from high dimensional observation signals. Our generative model had $d_x = 1$ and $d_y = 10$ and was of the form

$$\begin{aligned} \text{Latent Layer : } x_t &= \phi_x^\top(x_{t-1})\eta + u_t, \\ \text{Observations : } y_t^{[j]} &= \phi_y^\top(x_t)\theta^{[j]} + v_t^{[j]}, \end{aligned}$$

where $j = 1, \dots, 10$, $\phi_x^\top(x) = [\sin(\omega_x^\top x) \cos(\omega_x^\top x)]$ and $\phi_y^\top(x) = [\sin(\omega_y^\top x) \cos(\omega_y^\top x)]$. The elements of $\omega_x \in \mathbb{R}^{50}$ and $\omega_y \in \mathbb{R}^{50}$ were randomly generated from -10 to 10 , and the entries of $\eta \in \mathbb{R}^{100}$ and $\theta \in \mathbb{R}^{100}$ were also randomly drawn from -0.01 to 0.01 . The hyperparameters were set to be the same as in the above section. Figure 7 shows x_t and \hat{x}_t

of the last 100 samples. The results indicate that even when the signal shrinks and then enlarges suddenly, our model can adjust quickly and precisely.

C. Test on consistency of estimates

With this experiment, we compared the estimates by different members of an ensemble. We generated a one-dimensional latent process g_t as a GP with an RBF kernel with a hyperparameter length scale $l = 20$, and we created a latent process and observation processes according to

$$\begin{aligned} \text{Latent Layer : } x_t &= g_t + u_t, \\ \text{Observations : } y_t^{[1]} &= 1.2 \sin(x_t) - 0.5x_t + v_t^{[1]} \\ y_t^{[2]} &= 0.1x_t^3 - 0.7x_t + v_t^{[2]} \\ y_t^{[3]} &= 2x_t/(1 + x_t^2) + v_t^{[3]}, \end{aligned}$$

where the variances for u_t and v_t s were again 0.001 , and $J_x = J_y = 50$. Figure 8 presents five estimated latent processes \hat{x}_t (all plotted with grey color) obtained from different ensemble members. The true values of g_t are depicted

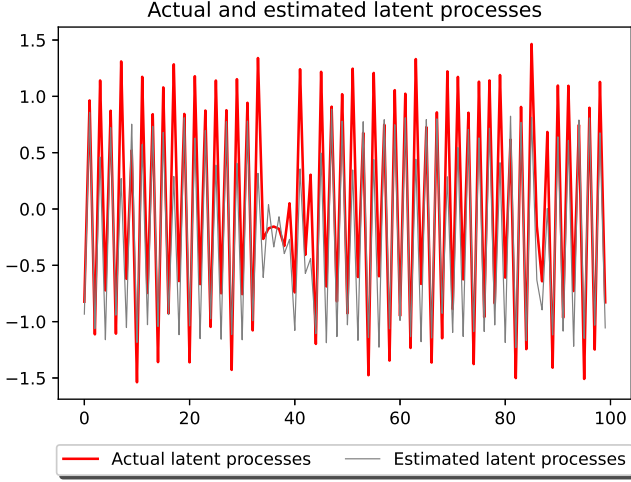


Fig. 7. Estimated latent process \hat{x}_t and actual latent process x_t .

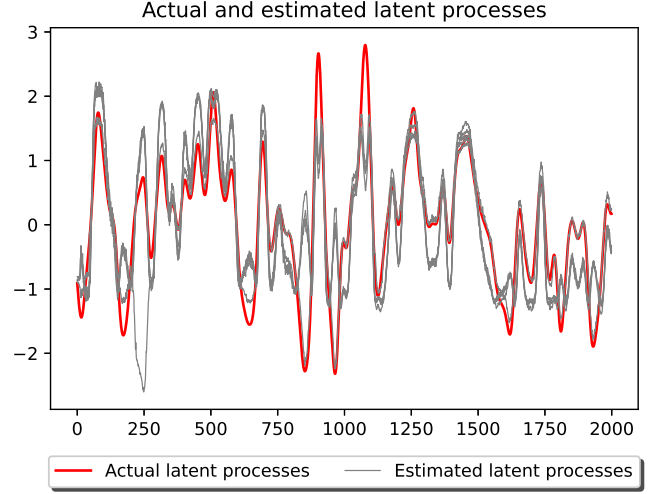


Fig. 8. Estimated latent process \hat{x}_t obtained with different seeds and the process g_t .

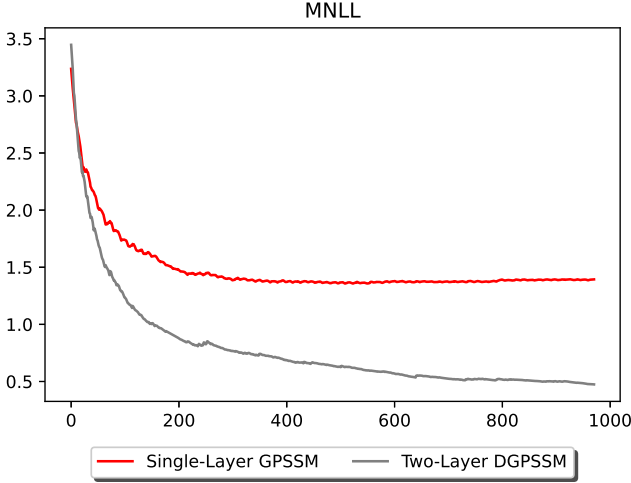


Fig. 9. MNLLs obtained from a single-layer GP-SSM and a two-layer GP-DSSM.

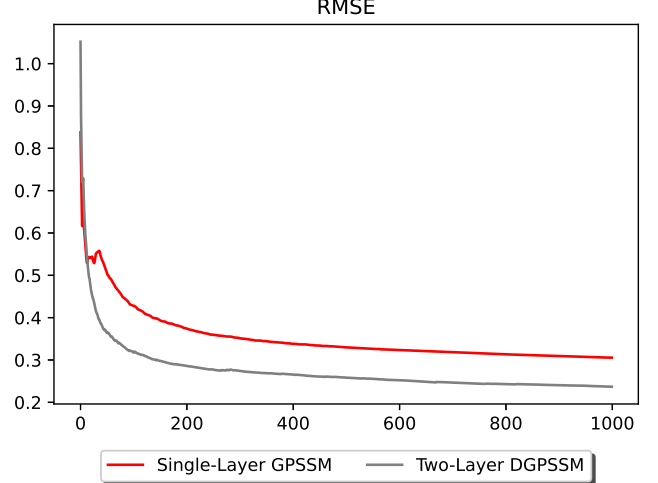


Fig. 10. RMSEs obtained from a single-layer GP-SSM and a two-layer GP-DSSM.

in red and compared with the estimated x_t . The results indicate that the members provided consistent results. We note that at around $t = 250$, there is a disagreement between the estimates. This time instant, however, belongs to the training period, which was from $t = 1$ to $T_0 = 1000$. During this period, the ensemble weights were fixed and equal. After T_0 , these weights varied according to the performance of the filters.

D. The need for a deep model

Do we need GP-DSSMs? This experiment shows that the answer is in general positive, especially when the selected kernel for the GP may not have enough capacity to learn. We validated this by an experiment where we reused the latent processes from Sec. VI-A. There $d_x = 2$ and $d_y = 1$. The difference was in the generation of the observation process. In the experiment, we generated the observation process as a GP whose kernel was a superposition of a dot-product and a white kernel. The dot-product kernel was a non-stationary kernel

with a hyper-parameter $\sigma_{dp}^2 = 20$ and the white kernel was white noise with $\sigma_v^2 = 0.001$. The outputs were normalized before being used by our model. In mathematical terms, the observation process was obtained by

$$y_t = f(x_t) + v_t, \quad (57)$$

where f is the GP with a dot-product kernel and v_t is the white kernel. The remaining parameters were $J_x = J_y = 50$. Figures 9 and 10 show the mean negative log-likelihoods (MNLLs) and the root mean square errors (RMSEs) of the two models. Clearly, the model with two layers captured the dot-product kernel significantly better than the ordinary GP-SSM.

E. Testing the performance of GP-DSSM

We generated data from a DSS model with two hidden layers, with $d_{x_1} = 2$, $d_{x_2} = 3$, and $d_y = 4$. The model is

Actual and estimated latent processes under the deep structure

Fig. 11. On the left are the true values and estimates of $\mathbf{x}_{1,t}$, and on the right, the true values and estimates of $\mathbf{x}_{2,t}$.

given by the following two layers of latent processes:

$$\begin{aligned}
 \text{Layer 1: } & x_{1,t}^{[1]} = 0.9x_{1,t-1}^{[1]} + 0.5\sin(x_{1,t-1}^{[1]}) + u_{1,t}^{[1]}, \\
 & x_{1,t}^{[2]} = 0.5\sin(x_{1,t-1}^{[1]}) + 0.9x_{1,t-1}^{[2]} + u_{1,t}^{[1]}, \\
 \\
 \text{Layer 2: } & x_{2,t}^{[1]} = 1.8\cos(x_{1,t}^{[1]}) - 0.7\sin(x_{1,t}^{[1]}) + u_{2,t}^{[1]}, \\
 & x_{2,t}^{[2]} = 0.5x_{1,t}^{[1]} - 1.3\sin(x_{1,t}^{[2]}) + u_{2,t}^{[1]}, \\
 & x_{2,t}^{[3]} = 2x_{1,t}^{[1]} - 0.4x_{1,t}^{[2]} + u_{2,t}^{[2]}
 \end{aligned} \tag{58}$$

and four observation processes given by

$$\begin{aligned}
 y_t^{[1]} &= 0.01(x_{2,t}^{[1]})^2 + 1.2x_{2,t}^{[3]} + v_t^{[1]}, \\
 y_t^{[2]} &= 1.2\sin(x_{2,t}^{[1]}) - 0.5x_{2,t}^{[2]} + 0.7x_{2,t}^{[3]} + v_t^{[2]}, \\
 y_t^{[3]} &= x_{2,t}^{[1]}x_{2,t}^{[2]} + v_t^{[3]}, \\
 y_t^{[4]} &= 5x_{2,t}^{[2]}/(1 + x_{2,t}^{[2]}) + v_t^{[4]}.
 \end{aligned} \tag{59}$$

This model is identical to the one from Sec. V-B of [43], except that we changed the first equation in [43]

$$x_{1,t}^{[1]} = 0.9x_{1,t-1}^{[1]} + 0.5\sin(x_{1,t-1}^{[2]}) + u_{1,t}^{[1]}, \tag{60}$$

to

$$x_{1,t}^{[1]} = 0.9x_{1,t-1}^{[1]} + 0.5\sin(x_{1,t-1}^{[1]}) + u_{1,t}^{[1]}. \tag{61}$$

We made this change to force the latent process to become less smooth, thus making it harder for estimation. The results are shown in Fig. 11. Evidently, they show that the proposed method is capable of accurately estimating all the latent processes even though the latent processes are much more jagged. Further, compared with the results in [43] which had persistent lags in the estimated processes, the results from the method presented here showed almost no lags.

VII. CONCLUSION

In this paper, we addressed the problem of sequential estimation of state-space models and deep state-space models using Gaussian process-based state-space modeling and Gaussian process-based deep state-space modeling. We implemented the Gaussian processes by using random feature-based Gaussian processes. The inference method is based on the combination of particle filtering and Bayesian linear regression. We also proposed an ensemble of filters for tracking the latent processes. With several experiments, we demonstrated the performance of the proposed method in different settings.

REFERENCES

- [1] J. Dean, D. Patterson, and C. Young, "A new golden age in computer architecture: Empowering the machine-learning revolution," *IEEE Micro*, vol. 38, no. 2, pp. 21–29, 2018.
- [2] I. Goodfellow, Y. Bengio, A. Courville, and Y. Bengio, *Deep Learning*. MIT Press Cambridge, 2016.
- [3] I. Katircioglu, B. Tekin, M. Salzmann, V. Lepetit, and P. Fua, "Learning latent representations of 3D human pose with deep neural networks," *International Journal of Computer Vision*, pp. 1–16, 2018.
- [4] W. Liu, Z. Wang, X. Liu, N. Zeng, Y. Liu, and F. E. Alsaadi, "A survey of deep neural network architectures and their applications," *Neurocomputing*, vol. 234, pp. 11–26, 2017.
- [5] M. Vatsa, R. Singh, and A. Majumdar, *Deep Learning in Biometrics*. CRC Press, 2018.
- [6] Y. Zhang, W. Chan, and N. Jaitly, "Very deep convolutional networks for end-to-end speech recognition," in *Acoustics, Speech and Signal Processing (ICASSP), 2017 IEEE International Conference on*. IEEE, 2017, pp. 4845–4849.
- [7] Y. Zhang, M. Pezeshki, P. Brakel, S. Zhang, C. L. Y. Bengio, and A. Courville, "Towards end-to-end speech recognition with deep convolutional neural networks," *arXiv preprint arXiv:1701.02720*, 2017.
- [8] K. He, X. Zhang, S. Ren, and J. Sun, "Deep residual learning for image recognition," in *Proceedings of the IEEE Conference on Computer Vision and Pattern Recognition*, 2016, pp. 770–778.
- [9] V. N. Murthy, S. Maji, and R. Manmatha, "Automatic image annotation using deep learning representations," in *Proceedings of the 5th ACM on International Conference on Multimedia Retrieval*. ACM, 2015, pp. 603–606.
- [10] A. Dutta, Y. Verma, and C. Jawahar, "Automatic image annotation: the quirks and what works," *Multimedia Tools and Applications*, pp. 1–21, 2018.
- [11] S. Schneider, G. W. Taylor, and S. C. Kremer, "Deep learning object detection methods for ecological camera trap data," *arXiv preprint arXiv:1803.10842*, 2018.
- [12] H. Chen, O. Engkvist, Y. Wang, M. Olivecrona, and T. Blaschke, "The rise of deep learning in drug discovery," *Drug Discovery Today*, 2018.
- [13] G. Urban, K. M. Bache, D. Phan, A. Sobrino, A. K. Shmakov, S. J. Hachey, C. Hughes, and P. Baldi, "Deep learning for drug discovery and cancer research: Automated analysis of vascularization images," *IEEE/ACM Transactions on Computational Biology and Bioinformatics*, 2018.
- [14] J. A. Diao, I. S. Kohane, and A. K. Manrai, "Biomedical informatics and machine learning for clinical genomics," *Human Molecular Genetics*, vol. 27, no. R1, pp. R29–R34, 2018.
- [15] A. Telenti, C. Lippert, P.-C. Chang, and M. DePristo, "Deep learning of genomic variation and regulatory network data," *Human Molecular Genetics*, vol. 27, no. R1, pp. R63–R71, 2018.
- [16] Y. Levine, O. Sharir, N. Cohen, and A. Shashua, "Bridging many-body quantum physics and deep learning via tensor networks," *arXiv preprint arXiv:1803.09780*, 2018.
- [17] R. Sharma, A. B. Farimani, J. Gomes, P. Eastman, and V. Pande, "Weakly-supervised deep learning of heat transport via physics informed loss," *arXiv preprint arXiv:1807.11374*, 2018.
- [18] C. E. Rasmussen and C. K. Williams, *Gaussian Processes for Machine Learning*. MIT press Cambridge, MA, 2006, vol. 2, no. 3.
- [19] M. Seeger, "Gaussian processes for machine learning," *International Journal of Neural Systems*, vol. 14, no. 02, pp. 69–106, 2004.
- [20] J. Quiñero Candela and C. E. Rasmussen, "A unifying view of sparse approximate Gaussian process regression," *The Journal of Machine Learning Research*, vol. 6, pp. 1939–1959, 2005.
- [21] E. Snelson and Z. Ghahramani, "Local and global sparse Gaussian process approximations," in *Artificial Intelligence and Statistics*. PMLR, 2007, pp. 524–531.
- [22] M. Titsias, "Variational learning of inducing variables in sparse Gaussian processes," in *Artificial intelligence and statistics*. PMLR, 2009, pp. 567–574.
- [23] T. Beckers and S. Hirche, "Prediction with approximated Gaussian process dynamical models," *IEEE Transactions on Automatic Control*, 2021.
- [24] R. Frigola, Y. Chen, and C. E. Rasmussen, "Variational Gaussian process state-space models," in *Advances in Neural Information Processing Systems*, 2014, pp. 3680–3688.
- [25] J. Kocijan, A. Girard, B. Banko, and R. Murray-Smith, "Dynamic systems identification with Gaussian processes," *Mathematical and Computer Modelling of Dynamical Systems*, vol. 11, no. 4, pp. 411–424, 2005.
- [26] D. Gedon, N. Wahlström, T. B. Schön, and L. Ljung, "Deep state space models for nonlinear system identification," *IFAC-PapersOnLine*, vol. 54, no. 7, pp. 481–486, 2021.
- [27] M. Fraccaro, "Deep latent variable models for sequential data," Ph.D. dissertation, PhD thesis, Technical University of Denmark, 2018.
- [28] S. S. Rangapuram, M. W. Seeger, J. Gasthaus, L. Stella, Y. Wang, and T. Januschowski, "Deep state space models for time series forecasting," *Advances in neural information processing systems*, vol. 31, pp. 7785–7794, 2018.
- [29] D. Salinas, V. Flunkert, J. Gasthaus, and T. Januschowski, "DeepAR: Probabilistic forecasting with autoregressive recurrent networks," *International Journal of Forecasting*, vol. 36, no. 3, pp. 1181–1191, 2020.
- [30] Y. Wang, A. Smola, D. Maddix, J. Gasthaus, D. Foster, and T. Januschowski, "Deep factors for forecasting," in *International conference on machine learning*. PMLR, 2019, pp. 6607–6617.
- [31] Z. Zhao, M. Emzir, and S. Särkkä, "Deep state-space Gaussian processes," *arXiv preprint arXiv:2008.04733*, 2020.
- [32] M. Deisenroth and J. W. Ng, "Distributed Gaussian processes," in *International Conference on Machine Learning*. PMLR, 2015, pp. 1481–1490.
- [33] E. Meeds and S. Osindero, "An alternative infinite mixture of Gaussian process experts," *Advances in Neural Information Processing Systems*, vol. 18, p. 883, 2006.
- [34] C. E. Rasmussen and Z. Ghahramani, "Infinite mixtures of Gaussian process experts," *Advances in Neural Information Processing Systems*, vol. 2, pp. 881–888, 2002.
- [35] V. Tresp, "Mixtures of Gaussian processes," *Advances in Neural Information Processing Systems*, pp. 654–660, 2001.
- [36] C. Yuan and C. Neubauer, "Variational mixture of Gaussian process experts," in *Advances in Neural Information Processing Systems*, 2009, pp. 1897–1904.
- [37] Q. Lu, G. Karanikolas, Y. Shen, and G. B. Giannakis, "Ensemble Gaussian processes with spectral features for online interactive learning with scalability," in *International Conference on Artificial Intelligence and Statistics*. PMLR, 2020, pp. 1910–1920.
- [38] M. Lázaro-Gredilla, J. Quinero-Candela, C. E. Rasmussen, and A. R. Figueiras-Vidal, "Sparse spectrum Gaussian process regression," *The Journal of Machine Learning Research*, vol. 11, pp. 1865–1881, 2010.
- [39] A. Zellner, *An Introduction to Bayesian Inference in Econometrics*. John Wiley & Sons, 1971.
- [40] P. M. Djurić, J. H. Kotecha, J. Zhang, Y. Huang, T. Ghirmai, M. F. Bugallo, and J. Míguez, "Particle filtering," *IEEE Signal Processing Magazine*, vol. 20, no. 5, pp. 19–38, 2003.
- [41] T. Li, M. Bolic, and P. M. Djurić, "Resampling methods for particle filtering: classification, implementation, and strategies," *IEEE Signal processing magazine*, vol. 32, no. 3, pp. 70–86, 2015.
- [42] G. Gundersen, M. Zhang, and B. Engelhardt, "Latent variable modeling with random features," in *International Conference on Artificial Intelligence and Statistics*. PMLR, 2021, pp. 1333–1341.
- [43] Y. Liu, M. Ajirak, and P. M. Djurić, "Inference with deep Gaussian process state space models," in *2022 30th European Signal Processing Conference (EUSIPCO)*. IEEE, 2022, pp. 792–796.